

1 A Additional Details for AutoBSS

2 A.1 Bayesian Optimization Based Search

3 In this procedure, we build a model for the accuracy of unevaluated BSSC based on evaluated one.
 4 Gaussian Process (GP, [1]) is a good method to achieve this in Bayesian optimization literature [2].
 5 A GP is a random process defined on some domain \mathcal{X} , and is characterized by a mean function
 6 $\mu : \mathcal{X} \rightarrow R$ and a covariance kernel $\kappa : \mathcal{X}^2 \rightarrow R$. In our method, $\mathcal{X} \in R^m$, where m is the dimension
 7 of BSSC.

8 Given $\mathcal{O} = \{(x^{(0)}, y^{(0)}), (x^{(1)}, y^{(1)}), \dots, (x^{(n-1)}, y^{(n-1)})\}$, where $x^{(i)}$ is a refined BSSC for an
 9 evaluated BSS, $y^{(i)}$ is the corresponding accuracy. We firstly standardize $y^{(i)}$ to $\hat{y}^{(i)}$ whose prior
 10 distribution has mean 0 and variance $1 + \eta^2$ so that $\hat{y}^{(i)}$ can be modeled as $\hat{y}^{(i)} = f(x^{(i)}) + \epsilon_i$, here f
 11 is a GP with $\mu(x) = 0$ and $\kappa(x, x') = \exp(-\frac{1}{2\sigma^2} \|x - x'\|_{L_2}^2)$, $\epsilon_i \sim N(0, \eta^2)$ is the white noise term,
 12 σ and η are hyperparameters. Considering that the variance of ϵ_i should be much smaller than the
 13 variance of $\hat{y}^{(i)}$, we simply set $\eta = 0.1$ in our method. σ determines the sharpness of the fall-off for
 14 kernel function $\kappa(x, x')$ and is determined dynamically based on the set \mathcal{O} , the details are illustrated
 15 below.

16 Firstly, we calculate the mean accuracy discrepancy for the BSSC evaluated in the first iteration. Be-
 17 cause they are dispersed clustering centers, the mean discrepancy is relatively large. Then, we utilize
 18 this value to filter \mathcal{O} and get the pairs of BSSC with a larger accuracy discrepancy than it. Afterward,
 19 we calculate the BSSC distance for the pairs and sort them to get $\{Dis_0, Dis_1, \dots, Dis_{l-1}\}$, where

20 $Dis_0 < Dis_1 < \dots < Dis_{l-1}$. Finally, σ is set as $\frac{Dis_{\frac{l}{20}}}{2}$.

21 It can be derived that the posterior process $f|\mathcal{O}$ is also a GP, we denote its mean function and
 22 kernel function as μ_n and κ_n respectively. Denote $Y \in R^n$ with $Y_i = \hat{y}^{(i)}$, $k, k' \in R^n$ with
 23 $k_i = \kappa(x, x^{(i)})$, $k'_i = \kappa(x', x^{(i)})$, and $K \in R^{n \times n}$ with $K_{i,j} = \kappa(x^{(i)}, x^{(j)})$. Then, μ_n, κ_n can be
 24 computed via,

$$\mu_n(x) = k^T (K + \eta^2 I)^{-1} Y, \quad \kappa_n(x, x') = \kappa(x, x') - k^T (K + \eta^2 I)^{-1} k'. \quad (1)$$

25 The value of posterior process $f|\mathcal{O}$ on each unevaluated BSS is a Gaussian distribution, whose mean
 26 and variance can be computed via equation 1. This distribution can measure the potential for each
 27 unevaluated BSSC. To determine the BSSC for evaluation, an acquisition function $\varphi : \mathcal{X} \rightarrow R$ is
 28 introduced, the BSSC with the maximum φ value will be selected. There are kinds of acquisitions [3],
 29 we use expected improvement (EI) in this work,

$$\varphi_{EI}(x) = \mathbb{E}(\max\{0, f(x) - \tau|\mathcal{O}\}), \tau = \max_{i < n} (\hat{y}^{(i)}). \quad (2)$$

30 EI measures the expected improvement over the current maximum value according to the posterior
 31 GP.

32 To reduce the time consumption and take advantage of parallelization, we train several different
 33 networks at a time. When selecting the first BSSC, equation 2 can be used directly. However,
 34 when selecting the following ones, there arises the problem that the accuracies for some BSSC are
 35 still unknown. Therefore, we use the expected value of EI function (EEL, [4]) instead. Supposing
 36 $x^{(n)}, x^{(n+1)}, \dots$ are BSSC for selected BSS with unknown accuracies $\tilde{y}^{(n)}, \tilde{y}^{(n+1)}, \dots$, thus

$$\varphi_{EEL}(x) = \mathbb{E}(\mathbb{E}(\max\{0, f(x) - \tau|\mathcal{O}, (x^{(n)}, \tilde{y}^{(n)}), (x^{(n+1)}, \tilde{y}^{(n+1)}), \dots\})), \quad (3)$$

37 here $\tilde{y}^{(n+j)}$ is a variable of Gaussian distribution with mean and variance depend on $\tilde{y}^{(n)}, \dots, \tilde{y}^{(n+j-1)}$.
 38 The value of equation 3 is calculated via Monte Carlo simulations [4] in our method.

39 B Additional Details for Experiments

40 B.1 Settings for the training networks on ImageNet

41 To study the performance of our method, a large number of networks are trained, including networks
42 with original BSS and the ones with sampled BSS. The specifics are shown in Table 1

Table 1: Settings for the training networks on ImageNet.

Shared	Optimizer:	SGD	Batch size:	1024
	Lr strategy:	Consin[6]	Label smooth:	0.1
	Weight decay	Initial Lr	Num of epochs	Augmentation
ResNet18	0.00004	0.4	120	-
ResNet50	0.0001	0.7	120	-
MobileNetV2	0.00002	0.7	120	-
EfficientNet-B0	0.00002	0.7	350	Fixed AutoAug[8]
EfficientNet-B1	0.00002	0.7	350	Fixed AutoAug[8]

43 B.2 Additional Details for the Definition of BSSC

44 B.2.1 Definition of BSSC for ResNet18/50 and MobileNetV2

45 The definition of BSSC for EfficientNet-B0/B1 has been introduced in paper. Here we demonstrate
the ones for ResNet18/50 and MobileNetV2.

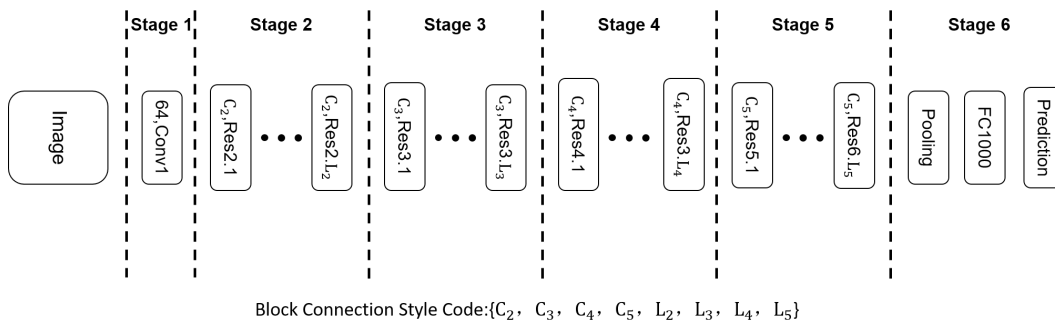


Figure 1: The backbone of ResNets. L_2, L_3, L_4, L_5 are number of blocks for each stage, C_2, C_3, C_4, C_5 are the corresponding output channels.

46

47 ResNet18/50 consists of 6 stages as illustrated in Figure 1. Stages 1~5 down-sample the spatial
48 resolution of input tensor, stage 6 produces the final prediction by a global average pooling and
49 a fully connected layer. The BSSC for ResNet18 is defined as the tuple $\{C_2, \dots, C_5, L_2, \dots, L_5\}$,
50 where C_i denotes the output channels, L_i denotes the number of residual blocks. As for the
51 BSSC of ResNet50, we utilize B_i to describe the bottleneck channels for stage i , thus it becomes
52 $\{C_2, \dots, C_5, L_2, \dots, L_5, B_2, \dots, B_5\}$.

53 MobileNetV2 consists of 9 stages, its main building block is mobile inverted bottleneck MBConv [9].
54 The specifics is shown in Table 2. In our experiment, the BSSC for MobileNetV2 is defined as the
55 tuple $\{C_3, \dots, C_8, L_3, \dots, L_8, T_3, \dots, T_8\}$. C_i, L_i and T_i denote the output channels, number of blocks
56 and expansion factor[9] for stage i respectively.

57 B.2.2 Constraints on the BSSC

58 For the BSSC of ResNet18, we constrain $\{C_2, \dots, C_5\}$ to be the power of 2, with the minimum
59 as $\{2^5, 2^5, 2^6, 2^7\}$ and maximum as $\{2^8, 2^{10}, 2^{11}, 2^{11}\}$. Moreover, the range of $L_i, i = 2, \dots, 5$
60 is constrained to be $[1, 16]$. For the BSSC of ResNet50, we constrain $\{C_2, \dots, C_5\}$ to be

Table 2: MobileNetV2 network. Each row describes a stage i with L_i layers, with input resolution $H_i \times W_i$, expansion factor[9] T_i and output channels C_i .

Stage i	Operator F_i	Resolution $H_i \times W_i$	Expansion factor T_i	Channels C_i	Layers L_i
1	Conv3x3	224×224	-	32	1
2	MBCConv,k3x3	112×112	1	16	1
3	MBCConv,k3x3	112×112	6	24	2
4	MBCConv,k3x3	56×56	6	32	3
5	MBCConv,k3x3	28×28	6	64	4
6	MBCConv,k3x3	14×14	6	96	3
7	MBCConv,k3x3	14×14	6	160	3
8	MBCConv,k3x3	7×7	6	320	1
9	Conv1x1&Pooling&FC	7×7	-	1280	1

61 the multiple of $\{64, 128, 256, 512\}$, with the minimum as $\{64, 128, 256, 512\}$ and maximum as
62 $\{320, 768, 1536, 3072\}$. $L_i, i = 2, \dots, 5$ are constrained to be no larger than 11. The value of B_i is
63 chosen from $\{\frac{C_i}{8}, \frac{C_i}{4}, \frac{3C_i}{8}, \frac{C_i}{2}\}$ for stage i .

64 For the BSSC of MobileNetV2, we constrain $\{C_3, \dots, C_8\}$ to be the multiple of $\{4, 8, 16, 24, 40, 80\}$,
65 with the minimum as $\{12, 16, 32, 48, 80, 160\}$ and maximum as $\{32, 64, 128, 192, 320, 640\}$.
66 $\{L_3, \dots, L_8\}$ are constrained to be no larger than $\{5, 6, 7, 6, 6, 4\}$. The value of expansion factor T_i is
67 chosen from $\{3, 6\}$.

68 For the BSSC of EfficientNet-B0/B1, we constrain $\{C_3, \dots, C_8\}$ to be the multiple
69 of $\{4, 8, 16, 28, 48, 80\}$, with the minimum as $\{16, 24, 48, 56, 144, 160\}$ and maximum as
70 $\{32, 64, 160, 280, 480, 640\}$. $\{L_3, \dots, L_8\}$ are constrained to be no larger than $\{6, 6, 7, 7, 8, 5\}$. The
71 value of expansion factor T_i is chosen from $\{3, 6\}$.

72 B.3 Additional Details for the Searched BSSC

73 B.3.1 The Searched BSSC on ImageNet

Table 3: Comparison between the original BSSC and the one searched by random search or our method.

Method	BSS Code	FLOPs	Params
ResNet18[10]	$\{64, 128, 256, 512, 2, 2, 2, 2\}$	1.81B	11.69M
ResNet18 ^{Rand}	$\{32, 64, 128, 512, 1, 2, 8, 5\}$	1.74B	24.87M
ResNet18 ^{AutoBSS}	$\{32, 32, 128, 1024, 4, 14, 14, 1\}$	1.81B	16.15M
ResNet50[10]	$\{256, 512, 1024, 2048, 3, 4, 6, 3, 64, 128, 256, 512\}$	4.09B	25.55M
ResNet50 ^{Rand}	$\{128, 640, 1024, 3072, 8, 7, 4, 3, 48, 80, 256, 384\}$	3.69B	23.00M
ResNet50 ^{AutoBSS}	$\{128, 256, 768, 2048, 9, 6, 9, 3, 48, 128, 192, 512\}$	4.03B	23.73M
MobileNetV2[11]	$\{24, 32, 64, 96, 160, 320, 2, 3, 4, 3, 3, 1, 6, 6, 6, 6, 6\}$	300M	3.50M
MobileNetV2 ^{Rand}	$\{20, 48, 80, 144, 200, 480, 2, 4, 3, 2, 5, 1, 3, 3, 3, 6, 3, 3\}$	298M	4.00M
MobileNetV2 ^{AutoBSS}	$\{24, 40, 64, 96, 120, 240, 4, 3, 2, 3, 6, 2, 3, 6, 6, 3, 6, 6\}$	296M	3.92M
EfficientNet-B0[11]	$\{24, 40, 80, 112, 192, 320, 2, 2, 3, 3, 4, 1, 6, 6, 6, 6, 6, 6\}$	385M	5.29M
EfficientNet-B0 ^{Rand}	$\{24, 40, 96, 112, 192, 640, 1, 2, 1, 2, 6, 1, 6, 6, 6, 3, 6, 6\}$	356M	6.67M
EfficientNet-B0 ^{AutoBSS}	$\{28, 48, 80, 140, 144, 240, 3, 1, 4, 2, 6, 3, 3, 3, 6, 3, 6, 6\}$	381M	6.39M
EfficientNet-B1[11]	$\{24, 40, 80, 112, 192, 320, 3, 3, 4, 4, 5, 2, 6, 6, 6, 6, 6, 6\}$	685M	7.79M
EfficientNet-B1 ^{Rand}	$\{16, 24, 128, 140, 240, 400, 4, 6, 2, 4, 5, 2, 3, 3, 3, 6, 6\}$	673M	10.19M
EfficientNet-B1 ^{AutoBSS}	$\{24, 64, 96, 112, 192, 240, 3, 1, 3, 4, 7, 5, 6, 3, 3, 3, 6, 6\}$	684M	10.17M

75

76 **B.3.2 The Searched BSSC on Model Compression**

Table 4: Comparison between the BSSC obtained by uniformly rescaling or AutoBSS for MobileNetV2.

Method	BSS Code	FLOPs	Params
Uniformly Rescale	{16,20,40,56,96,192,2,3,4,3,3,1,6,6,6,6,6}	130M	2.2M
AutoBSS(ours)	{16,20,40,56,96,288,1,4,6,1,6,1,3,6,6,3,6,6}	130M	2.7M

77 **B.3.3 The Searched BSSC on Detection and Instance Segmentation**

Table 5: Comparison between the original BSS and the one searched by AutoBSS.

Backbone	BSS Code	FLOPs	Params
Mask R-CNN-R50	{256,512,1024,2048,3,4,6,3,64,128,256,512}	117B	44M
Mask R-CNN-R50 ^{AutoBSS}	{192,512,512,1024,9,3,6,10,24,192,256,384}	116B	49M
RetinaNet-R50	{256,512,1024,2048,3,4,6,3,64,128,256,512}	146B	38M
RetinaNet-R50 ^{AutoBSS}	{192,384,768,1536,3,7,9,8,72,192,192,384}	146B	41M

78 **B.4 Additional Details for Settings on Detection and Instance Segmentation**

79 We train the models on COCO [12] train2017 split, and evaluate on the 5k COCO val2017 split. We
80 evaluate bounding box (bbox) Average Precision (AP) for object detection and mask AP for instance
81 segmentation.

82 **Experiment settings** Most settings are identical with the ones on ImageNet classification task,
83 we only introduce the task specific settings here. We adopt the end-to-end fashion [13] of training
84 Region Proposal Networks (RPN) jointly with Mask R-CNN. All models are trained from scratch
85 with 8 GPUs, with a mini-batch size of 2 images per GPU. We train a total of 270K iterations.
86 SyncBN [14] is used to replace all 'frozen BN' layers. The initial learning rate is 0.02 with 2500
87 iterations to warm-up [5], and it will be reduced by $10\times$ in the 210K and 250K iterations. The weight
88 decay is 0.0001 and momentum is 0.9. Moreover, no data augmentation is utilized for testing, and
89 only horizontal flipping augmentation is utilized for training. The image scale is 800 pixels for the
90 shorter side for both testing and training. The BSSC is defined as the one for ResNet50 on ImageNet
91 classification task and we also constrain the FLOPs for the searched BSS no larger than the original
92 one. FLOPs is calculated with an input size 800×800 . Only backbone, FPN and RPN are taken into
93 account for the FLOPs of Mask R-CNN-R50. In the searching procedure, we only target to search
94 BSS for higher AP.

95 **References**

- 96 [1] Carl Edward Rasmussen. Gaussian processes in machine learning. In *Summer School on*
97 *Machine Learning*, pages 63–71. Springer, 2003.
- 98 [2] James S Bergstra, Rémi Bardenet, Yoshua Bengio, and Balázs Kégl. Algorithms for hyper-
99 parameter optimization. In *Advances in neural information processing systems*, pages 2546–
100 2554, 2011.
- 101 [3] Eric Brochu, Vlad M. Cora, and Nando de Freitas. A tutorial on bayesian optimization of
102 expensive cost functions, with application to active user modeling and hierarchical reinforcement
103 learning. *CoRR*, abs/1012.2599, 2010.
- 104 [4] David Ginsbourger, Janis Janusevskis, and Rodolphe Le Riche. Dealing with asynchronicity
105 in parallel Gaussian Process based global optimization. Research report, Mines Saint-Etienne,
106 2011.
- 107 [5] Priya Goyal, Piotr Dollár, Ross Girshick, Pieter Noordhuis, Lukasz Wesolowski, Aapo Kyrola,
108 Andrew Tulloch, Yangqing Jia, and Kaiming He. Accurate, large minibatch sgd: Training
109 imagenet in 1 hour. *arXiv preprint arXiv:1706.02677*, 2017.
- 110 [6] Tong He, Zhi Zhang, Hang Zhang, Zhongyue Zhang, Junyuan Xie, and Mu Li. Bag of tricks for
111 image classification with convolutional neural networks. In *The IEEE Conference on Computer*
112 *Vision and Pattern Recognition (CVPR)*, June 2019.
- 113 [7] Gao Huang, Yu Sun, Zhuang Liu, Daniel Sedra, and Kilian Q Weinberger. Deep networks with
114 stochastic depth. In *European conference on computer vision*, pages 646–661. Springer, 2016.
- 115 [8] Ekin D Cubuk, Barret Zoph, Dandelion Mane, Vijay Vasudevan, and Quoc V Le. Autoaugment:
116 Learning augmentation strategies from data. In *Proceedings of the IEEE conference on computer*
117 *vision and pattern recognition*, pages 113–123, 2019.
- 118 [9] Mark Sandler, Andrew Howard, Menglong Zhu, Andrey Zhmoginov, and Liang-Chieh Chen.
119 Mobilenetv2: Inverted residuals and linear bottlenecks. In *The IEEE Conference on Computer*
120 *Vision and Pattern Recognition*, pages 4510–4520, 2018.
- 121 [10] Kaiming He, Xiangyu Zhang, Shaoqing Ren, and Jian Sun. Deep residual learning for image
122 recognition. In *The IEEE conference on computer vision and pattern recognition*, pages
123 770–778, 2016.
- 124 [11] Mingxing Tan and Quoc V. Le. Efficientnet: Rethinking model scaling for convolutional neural
125 networks. In *International Conference on Learning Representations*, pages 6105–6114, 2019.
- 126 [12] Tsung-Yi Lin, Michael Maire, Serge Belongie, James Hays, Pietro Perona, Deva Ramanan, Piotr
127 Dollár, and C Lawrence Zitnick. Microsoft coco: Common objects in context. In *European*
128 *conference on computer vision*, pages 740–755. Springer, 2014.
- 129 [13] Shaoqing Ren, Kaiming He, Ross Girshick, and Jian Sun. Faster r-cnn: Towards real-time
130 object detection with region proposal networks. In *Advances in neural information processing*
131 *systems*, pages 91–99, 2015.
- 132 [14] Chao Peng, Tete Xiao, Zeming Li, Yuning Jiang, Xiangyu Zhang, Kai Jia, Gang Yu, and Jian
133 Sun. Megdet: A large mini-batch object detector. In *Proceedings of the IEEE Conference on*
134 *Computer Vision and Pattern Recognition*, pages 6181–6189, 2018.